

Reduction of 2-(*N,N*-dimethylamino)ethyl substituted zirconocene dichlorides: Intramolecular activation of NCH₂–H bond. The crystal structures of $[\eta^5:\eta^2(C,N)\text{-C}_5(\text{CH}_3)_4\text{CH}_2\text{CH}_2\text{N}(\text{CH}_3)\text{CH}_2][\eta^5\text{-C}_5(\text{CH}_3)_5]\text{ZrX}$ (X = Cl, H)

Dmitrii P. Krut'ko^{a,*}, Maxim V. Borzov^a, Roman S. Kirsanov^a,
Andrei V. Churakov^b, Lyudmila G. Kuz'mina^b

^a Department of Chemistry, M.V. Lomonosov Moscow State University, GSP-2, Leninskie Gory 1, bldg. 3, Moscow 119992, Russian Federation

^b N.S. Kurnakov Institute of General and Inorganic Chemistry, Russian Academy of Sciences, Leninskii prosp. 31, Moscow 119991, Russian Federation

Received 12 July 2004; revised 2 March 2005; accepted 2 March 2005

Available online 23 May 2005

Abstract

Treatment of zirconocene dichloride $[\eta^5\text{-C}_5(\text{CH}_3)_4\text{CH}_2\text{CH}_2\text{N}(\text{CH}_3)_2][\eta^5\text{-C}_5(\text{CH}_3)_5]\text{ZrCl}_2$ (**1**) with amalgamated magnesium in THF results in cleavage of a C–H bond in one of the methyl groups of the N(CH₃)₂ fragment yielding $[\eta^5:\eta^2(C,N)\text{-C}_5(\text{CH}_3)_4\text{CH}_2\text{CH}_2\text{N}(\text{CH}_3)\text{CH}_2][\eta^5\text{-C}_5(\text{CH}_3)_5]\text{ZrH}$ (**2**). An analogous reduction of $[\eta^5\text{-C}_5(\text{CH}_3)_4\text{CH}_2\text{CH}_2\text{N}(\text{CH}_3)_2]\text{ZrCl}_2$ (**4**) proceeds similarly only in the presence of great excess of P(CH₃)₃, otherwise no identifiable products are formed. Heterogeneous reaction of the hydride complex **2** with NH₄Cl in THF produces the corresponding chloride complex $[\eta^5:\eta^2(C,N)\text{-C}_5(\text{CH}_3)_4\text{CH}_2\text{CH}_2\text{N}(\text{CH}_3)\text{CH}_2][\eta^5\text{-C}_5(\text{CH}_3)_5]\text{ZrCl}$ (**3**), with the Zr–CH₂ bond retained. The molecular structures of compounds **2** and **3** were established by X-ray diffraction analyses.

© 2005 Elsevier B.V. All rights reserved.

Keywords: Zirconium; Cyclopentadienyl ligands; Oxidative addition; Reduction; N ligands

1. Introduction

Recently, we reported the preparation of $[\eta^5\text{-C}_5(\text{CH}_3)_4\text{CH}_2\text{CH}_2\text{N}(\text{CH}_3)_2][\eta^5\text{-C}_5(\text{CH}_3)_5]\text{ZrCl}_2$ (**1**) and $[\eta^5\text{-C}_5(\text{CH}_3)_4\text{CH}_2\text{CH}_2\text{N}(\text{CH}_3)_2]\text{ZrCl}_2$ (**4**) [1]. As well as it was done previously for $[\eta^5\text{-C}_5(\text{CH}_3)_4\text{CH}_2\text{CH}_2\text{ECH}_3][\eta^5\text{-C}_5(\text{CH}_3)_5]\text{ZrCl}_2$ (E = O, S) [2], we have studied the reduction reactions of **1** and **4** under similar conditions (amalgamated magnesium in THF). Here, we present these results along with the discussion of the dramatic difference in the reduction behavior of **1** and **4** and their O- and S-analogues.

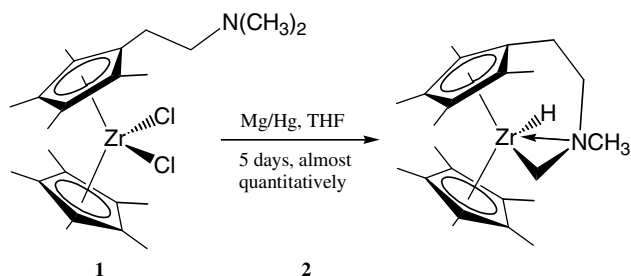
2. Results and discussion

2.1. Reduction of zirconocene dichloride **1** with amalgamated magnesium

Treatment of the initial zirconocene dichloride $[\eta^5\text{-C}_5(\text{CH}_3)_4\text{CH}_2\text{CH}_2\text{N}(\text{CH}_3)_2][\eta^5\text{-C}_5(\text{CH}_3)_5]\text{ZrCl}_2$ (**1**) with amalgamated magnesium in THF at room temperature results in appearance of a dark-brown coloration of the reaction mixture, that gradually discharges and in 5 days (room temperature) the solution becomes virtually colorless. NMR monitoring of the reaction mixture indicates that the reaction proceeds unambiguously as it is presented in Scheme 1.

On removal of the solvent, extraction of the residue with benzene followed by recrystallization from ether,

* Corresponding author. Tel.: +7 95 939 1234; fax: +7 95 932 8846.
E-mail address: kdp@org.chem.msu.su (D.P. Krut'ko).



Scheme 1.

complex **2** was isolated in $\sim 70\%$ yield as a colorless crystalline solid.

The structure of the alkylhydride zirconium complex **2** in a solution was established by means of ^1H and ^{13}C NMR spectroscopy. The ^1H NMR spectrum of **2** is presented in Fig. 1. To prove the spatial structure of **2** in a solution, a series of NOE difference experiments was carried out. In Fig. 1, the selected NOE enhancement values are also depicted.

The measurements of the NOE enhancement values, with protons Zr-H , $\text{CH}_3(5)$, $\text{CH}_3(4)$, NCH_3 , $\text{H}(8a)$ and $\text{H}(8b)$ consecutively irradiated, made it possible to perform the complete assignment of the signals in the NMR spectra and to determine the conformation of

the $\text{Zr-C}(1)\text{-C}(6)\text{-C}(7)\text{-N-C}(8)\text{-(Zr)}$ framework metallacycle as a one resembling a pseudo-six-member boat. These NMR spectroscopy data for complex **2** in a solution are in an excellent agreement with the X-ray diffraction analysis data (vide infra). The hydride atom is in a close neighborhood to $\text{CH}_3(5)$ moiety and for this methyl group in both ^1H and coupled ^{13}C NMR spectra distinct through-space spin–spin coupling is observed ($J(\text{H-ZrH}) = 1.6 \text{ Hz}$, $J(\text{C-ZrH}) = 6.5 \text{ Hz}$). A selective decoupling from the $(\text{Zr})\text{-H}$ hydride atom causes a collapse of the $\text{CH}_3(5)$ doublet.

The coordination of the nitrogen atom in crystalline state was proved by X-ray diffraction analysis data (vide infra). In a solution, this coordination is also retained. This is evident because of the distinct deshielding of the $\text{CH}_2(7)$ and NCH_3 carbons comparatively to zirconocene dichloride **1** [1]: $\delta(\text{CH}_2(7)) = 68.43$ vs. 60.13 ppm for **1** and $\delta(\text{NCH}_3) = 52.39$ vs. 45.75 ppm for **1**. The increase of the direct spin–spin coupling constants is also noteworthy: $^1J(^{13}\text{CH}_2(7)\text{-}^1\text{H}) = 137$ vs. 133 Hz (for **1**) and $^1J(^{13}\text{CH}_3\text{N-}^1\text{H}) = 136$ vs. 132 Hz (for **1**).

We examined a series of reactions of complex **2** (see Scheme 2).

Addition of excess of tertiary phosphanes to zirconocene alkylhydrides was reported to cause evolution of corresponding alkanes and formation of divalent

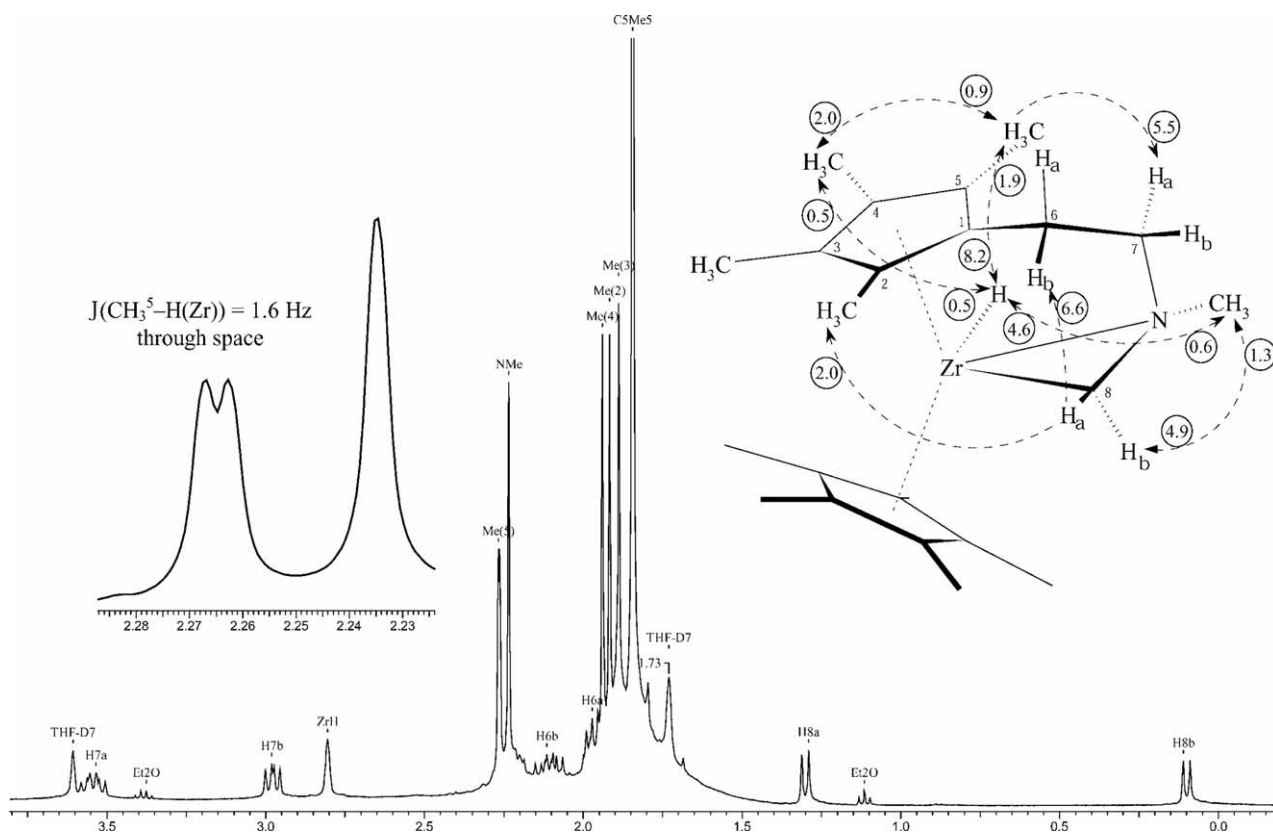
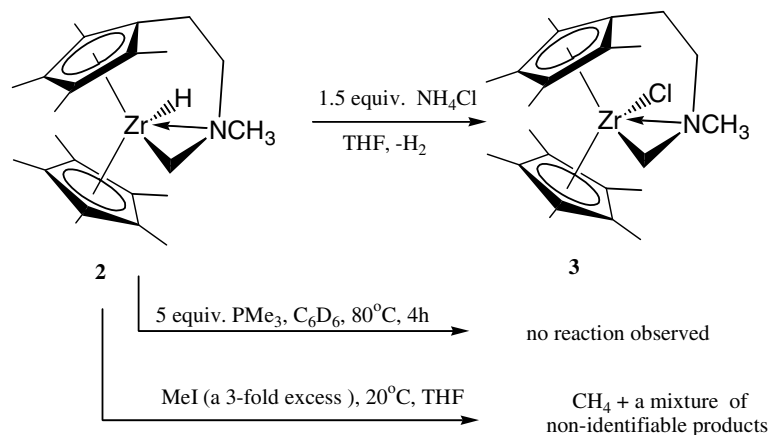


Fig. 1. ^1H NMR spectrum of complex **2**, the preferable “boat” conformation of the $\text{Zr-C}(1)\text{-C}(6)\text{-C}(7)\text{-N-C}(8)\text{-(Zr)}$ six-member pseudo-metallacycle, and the selected NOE enhancements (%) for remote by chain, but sterically close protons.



zirconocene diphosphanes $\text{Cp}_2\text{Zr}(\text{PR}_3)_2$ [3,4]. In our case, however, this does not happen and treatment of **2** with a 5-fold excess of PMe_3 gives no effect. The stability of alkylhydride complex **2** is due to the coordination of the nitrogen atom towards the Zr(IV) center that separates hydride and alkyl ligands and, this way, prevents the reductive elimination to occur. In addition, complex **2** is an 18-electron one, with all of the coordination places occupied. This also contributes into the decrease of its reactivity in the ligand exchange reactions by the association–dissociation mechanism.

On the other hand, reactions of **2** with CH_3I and NH_4Cl reveal the high lability of the hydride atom. In the first case, an instant evolution of methane ($\delta(^1\text{H}) = 0.19$ ppm, THF-d_8) was observed. Unfortunately, we failed to stop the process at this stage and as a result a mixture of unidentified products formed. Most likely, the further attack of CH_3I proceeds at the nitrogen atom that causes its quaternation, liberation of one of the coordination positions and the subsequent reactions at the metal atom.

Heterogeneous interaction of **2** and a 1.5 mol excess of NH_4Cl unambiguously gives the only zirconocene alkylchloride type complex **3** that was isolated in a good yield (~70%, crystallization from diethyl ether). Markedly, the Zr– CH_2 bond in **2** retains and no initial zirconocenedichloride **1** is observed in the reaction mixture. This reaction processes not instantly due to its heterogeneous character. Thus, in one of the runs, the unreacted **2** and product **3** co-crystallized yielding single crystals acceptable for the X-ray diffraction analysis (all attempts to grow up a single crystal of pure **2** suitable for X-ray analysis failed).

The similarity of the appearance of the ^1H and ^{13}C NMR spectra of complexes **3** and **2** indicates the similarity of their spatial structure in solutions. Of course, replacement of Cl for H eliminates the through-space coupling of the hydride atom and CH_3 (5) group. So, in ^1H and coupled ^{13}C NMR spectra no additional splitting is observed.

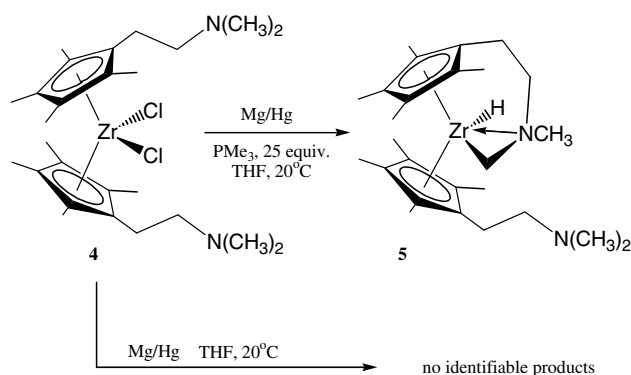
2.2. Reduction of zirconocenedichloride **4**

Surprisingly, reduction of the bis(*N,N*-dimethylaminoethyl) substituted zirconocenedichloride **4** under the same reaction conditions as employed for **1** gave no identifiable products (see Scheme 3), with the dark-brown coloration of the reaction mixture not discharged. However, if performed at the presence of a great (25-fold) excess of PMe_3 , the course of the reduction is analogous to that for **1** and after removal of the volatiles, extraction with benzene and recrystallization from hexane zirconocene alkylhydride **5** was isolated in a good (~60%) yield.

The ^1H and ^{13}C NMR spectra for **5**, actually, present a superposition of those for **2** and **4**, with only the signals related to the C_5Me_5 moiety being absent. Thus, the spatial structures of the $\eta^5\text{-C}_5\text{Me}_4\text{-CH}_2\text{CH}_2\text{-N}(\rightarrow\text{Zr})\text{-CH}_2\text{-Zr}$ frameworks in **2** and **5** are similar.

2.3. X-ray structural studies of complexes **2** and **3**

The structure of compound **3** was established by X-ray diffraction analyses. Molecular geometry and numbering scheme for **3** is shown in Fig. 2, selected bond lengths and angles are listed in Table 1.



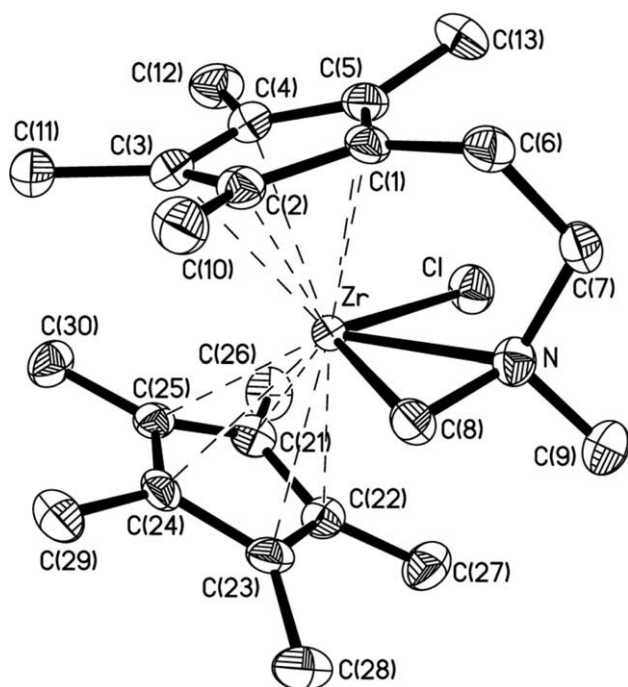


Fig. 2. Molecular structure of **3**. Displacement ellipsoids are shown at 50% probability level. Hydrogen atoms are omitted for clarity.

Table 1
Selected bond lengths (Å) and angles (°) for **3** and co-crystallized **2** and **3**

	3	Co-crystallized 2 and 3
Zr–Cl	2.551(1)	2.631(3)
Zr–H	–	1.63(5)
Zr–N	2.314(4)	2.314(2)
Zr–C(8)	2.297(4)	2.305(3)
Zr–Cp(1) ^a	2.251	2.240
Zr–Cp(2) ^b	2.298	2.267
N–C(8)	1.466(5)	1.467(4)
N–C(7)	1.483(5)	1.482(4)
Cl–Zr–N	80.30(9)	80.17(9)
Cl–Zr–C(8)	115.9(1)	115.7(1)
H–Zr–N	–	73(2)
H–Zr–C(8)	–	109(2)
N–Zr–C(8)	37.1(1)	37.05(9)
Cp(1)–Zr–Cp(2)	135.8	137.5
C(8)–N–Zr	70.8(2)	71.2(2)
C(7)–N–Zr	117.8(3)	118.0(2)
C(8)–N–C(7)	117.9(3)	116.2(2)
N–C(8)–Zr	72.1(2)	71.8(2)

^a Cp(1) denotes the center of functionalized Cp-ring.

^b Cp(2) denotes the center of pentamethyl Cp-ring.

Compound **3** represents a bent metallocene sandwich. The value of Cp(cent)–Zr–Cp(cent) angle (135.8°) compares well with those found for (C₅Me₅)₂Zr(OH)Cl – 137.9° [5] and (C₅Me₅)(C₅Me₄CH₂CH₂NMe₂)ZrCl₂ – 136.9° [1]. Both cyclopentadienyl rings are planar within 0.023(3) Å. As expected [6], nine methyl(Cp) substituents deviate slightly from the least-squares planes of the Cp-rings in the direction opposite to the Zr atom

(0.092(8)–0.369(8) Å). Maximal distortions were observed for C(11) and C(30) atoms forming short intramolecular contact (3.215(7) Å). However, C(6) atom is shifted towards the Zr atom (0.100(7) Å). The latter is probably caused by the steric requirements of the constrained –Zr–C(1)–C(6)–C(7)–N(→Zr) metallacycle. This also causes the decrease of Cp(cent)–Zr distance for functionalized Cp-ring (2.251 Å) in comparison to that for the pentamethylcyclopentadienyl one – 2.298 Å. Analysis of the Cambridge Structural Database (Release: January 2004) [7] shows that the Zr–Cl distance (2.551(1) Å) is within the normal range for terminal Zr–Cl bonds in bicyclopentadienyl complexes (2.343–2.646 Å, 585 entries). Chlorine atom and nitrogen and C(8) atoms of η²-CN moiety lie approximately in the plane bisecting CpZrCp unit (mean deviation is 0.12 Å). Nitrogen occupies the central coordination site, while methylene group lies in the lateral position. The geometrical parameters of the three-membered metallacycle Zr–N–C(8) are very similar to those found for closely related complex Cp₂Zr(η²-NMe₂CHPh)(CF₃CO₂) [8]. This structural motif was established for a number of cyclopentadienyl Ti(IV) and Zr(IV) complexes [9–12].

Compound **2** is isostructural with **3**. The single crystal subjected to the X-ray diffraction analysis represents co-crystallized chlorine and hydrido derivatives of one and the same metallocene core (**3** and **2**, respectively) in 0.25:0.75 ratio (see Fig. 3).

The molecular geometry of the co-crystallized **2** and **3** is very close (see Table 1). Orthogonal fitting based on all non-hydrogen atoms except partially occupied chlorines led to r.m.s. deviation 0.106 Å. In the structure

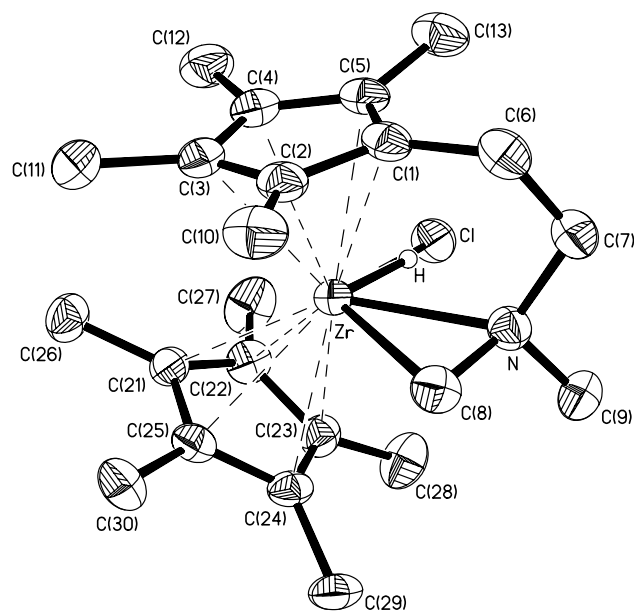


Fig. 3. Molecular structure of co-crystallized **2** and **3**. Displacement ellipsoids are shown at 50% probability level. Hydrogen atoms (except hydride H) are omitted for clarity.

of the subunit **3** in co-crystallized **2** and **3**, Zr–Cl distance is somewhat longer than observed for the pure **3** (vide supra) due to the disordering of the chlorine atom in the crystal of the co-crystallized **2** and **3**. The Zr–H bond length (1.63(5) Å) is comparable with some other previously reported terminal Cp₂Zr–H distances (1.68(8), 1.78(2) Å [13,14]).

2.4. Comparison of the reactions of **1** and **4** with Mg/Hg with those of their O- and S-analogues

It is a known fact that the Group 4 metallocene dihalides, if treated with an appropriate reagent in presence of a side ligand that exhibits both *n*-donor and, at least weak, π -acidic properties (CO, tertiary phosphanes or even N₂) can be reduced to the divalent metal complexes [15–20]. However, in absence of such stabilizer and even in case of its low concentration, complexes of the divalent metal eagerly convert to the M(III) compounds [3,4,21]. This conversion usually occurs as an insertion of the coordination-deficient metal center into a C–H [15,17,20,22] or C–heteroelement bond [2] (i.e., oxidative addition reaction) and may process in both inter- or intramolecular fusion.

Remarkably, that the results on the reduction behavior of complexes **1** and **4** dramatically differ from the previously reported ones for $[\eta^5\text{-C}_5(\text{CH}_3)_4\text{CH}_2\text{CH}_2\text{ECH}_3]\text{ZrCl}_2$ ($E = \text{O}, \text{S}$) [2] (see Scheme 4).

In cases of $[\eta^5\text{-C}_5(\text{CH}_3)_4\text{CH}_2\text{CH}_2\text{ECH}_3][\eta^5\text{-C}_5(\text{CH}_3)_5]\text{ZrCl}_2$ ($E = \text{O}, \text{S}$) treatment with Mg/Hg in THF caused the cleavage of the E–Me bond, while in case of complex **1** one of the C–H bonds of the NMe₂ group is split.

The changes in coloration within the course of the reaction allow one to suspect that the formation of the Zr(IV) compound **2** involves a low-valent Zr intermediate, presumably of Zr(II) nature. As a matter of fact, the

visible changes of the reaction mixtures for the cases of O- and S-analogues of **1** and **4** are quite alike. From the same viewpoint, one can also suppose that the role PMe₃ plays in changing the course of the reduction of **4** is to reversibly stabilize the believed Zr(II) intermediate and to prevent coordination of the second NMe₂ group to the metal center.

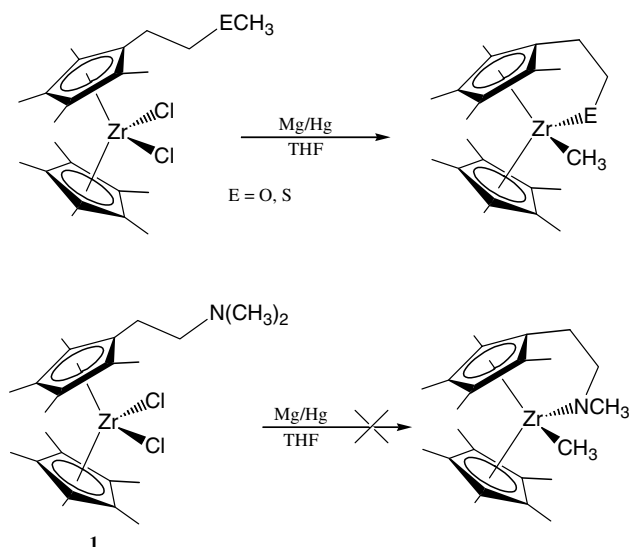
The reactions of question mechanistically could be related to the reduction–oxidative addition type. Such a dramatic difference between the results of the reductions of CH₃E– ($E = \text{O}, \text{S}$) and (CH₃)₂N– side-chain functionalized zirconocene dichlorides may be accommodated if one assumes that in the low-valent Zr intermediate the heteroatom functionality coordinates to this high-reactive metal center. On the next elementary stage, it is the most favorably oriented towards the metal center bond that undergoes the oxidative addition. However, the true reasons that determine the regioselectivity in the cases of interest need, of course, further detailed investigations, possibly with application of the quantum-chemical modeling.

Of interest, a product of intramolecular NCH₂–H bond cleavage similar in appearance but markedly different in nature and origin to complexes **1** and **5** was observed by Erker and co-workers [11]. In the cited paper, the cationic complex $[\eta^5:\eta^2(\text{C},\text{N})\text{-C}_5\text{H}_4\text{C}(\text{CH}_3)_2\text{N}(\text{CH}_3)\text{CH}_2](\eta^5\text{-C}_5\text{H}_5)\text{Zr}^+$ was formed from dimethyl zirconocene $[\eta^5\text{-C}_5\text{H}_4\text{C}(\text{CH}_3)_2\text{N}(\text{CH}_3)_2](\eta^5\text{-C}_5\text{H}_5)\text{Zr}(\text{CH}_3)_2$ on treatment with B(C₆F₅)₃ via unstable cationic intermediate $[\eta^5:\eta^1\text{-N-C}_5\text{H}_4\text{C}(\text{CH}_3)_2\text{N}(\text{CH}_3)_2](\eta^5\text{-C}_5\text{H}_5)\text{-Zr}(\text{CH}_3)^+$ by a spontaneous methane elimination reaction. In this case, the Zr-center possesses a d⁰-configuration and, actually, there is no evidence that the methane formation includes, as an elementary step, an oxidative addition of a C–H bond.

3. Experimental

3.1. General remarks

All procedures were performed in sealed-off evacuated glass vessels. The employed solvents (and their per-deuterated analogues) were dried with and distilled from conventional agents (namely diethyl ether and THF with sodium benzophenone ketyl, benzene and hexane with Na–K alloy, CH₃I with P₂O₅ and then with CaH₂). When performing procedures in evacuated vessels, the degassed solvents were stored in evacuated reservoirs over corresponding drying agent and transferred on a high vacuum line directly into reaction vessels by trapping them with liq. N₂. NH₄Cl was sublimed under high vacuum conditions prior to use. P(CH₃)₃ was prepared and dozed by quantitative thermolysis of [IAg(P(CH₃)₃)₄] [23] under high-vacuum conditions and trapping it with liq. N₂ directly into a reaction



Scheme 4.

vessel. Amalgamated magnesium [2], $[\eta^5\text{-C}_5(\text{CH}_3)_4\text{CH}_2\text{CH}_2\text{N}(\text{CH}_3)_2][\eta^5\text{-C}_5(\text{CH}_3)_5\text{ZrCl}_2$ (**1**) and $[\eta^5\text{-C}_5(\text{CH}_3)_4\text{CH}_2\text{CH}_2\text{N}(\text{CH}_3)_2]\text{ZrCl}_2$ (**4**) were prepared accordingly to the reported procedure [1]. ^1H and ^{13}C NMR spectra were recorded on a Varian VXR-400 spectrometer at 400 and 100 MHz, respectively. For ^1H and ^{13}C spectra, the solvent resonances [$\delta_{\text{H}} = 7.15$ and $\delta_{\text{C}} = 128.0$ (C_6D_6), $\delta_{\text{H}} = 1.73$ and $\delta_{\text{C}} = 25.3$ (THF-d_8)] were used as internal reference standards. Mass spectra were measured on Kratos-MS-890 spectrometer. The elemental analyses were performed on the Carlo-Erba automated analyser.

3.2. NMR-monitored reactions (general technique)

A 5 mm diameter NMR tube was charged under high vacuum with a corresponding complex and a reactant (Mg/Hg , NH_4Cl). If the required reactant was a volatile compound (CH_3I , $\text{P}(\text{CH}_3)_3$), it was transferred into the tube on a high-vacuum line by trapping with liq. N_2 . To this mixture cooled down to the liq. N_2 temperature, THF-d_8 was transferred on the line, the NMR tube sealed off, the reaction mixture thawed and allowed to warm up to room temperature.

3.3. $[\eta^5:\eta^2(C,N)\text{-C}_5(\text{CH}_3)_4\text{CH}_2\text{CH}_2\text{N}(\text{CH}_3)\text{CH}_2\text{-}][\eta^5\text{-C}_5(\text{CH}_3)_5\text{ZrH}$ (**2**)

A solution of **1** (400 mg, 0.817 mmol) in THF (20 ml) was stirred with Mg/Hg (250 mg, 10.4 mmol) during 5 days. Reaction starts after 10–30 min after mixing the reactants (dark reddish-brown coloration). At the end the mixture becomes virtually colorless. On filtering from Mg , removal of the solvent and drying on the high-vacuum line, the residue was taken with benzene (10 ml), filtered from MgCl_2 , and concentrated to dryness. Brownish-white crystalline solid. The yield of the crude product is nearly quantitative. Recrystallization from diethyl ether (5 ml) gave pure **2** as colorless crystals (229 mg, 0.547 mmol, 67%). ^1H NMR (25 °C, THF-d_8): $\delta = 0.10$ (d, 1H, $^2J_{\text{HH}} = 8.8$ Hz, $\text{H}^{8\text{b}}$), 1.30 (d, 1H, $^2J_{\text{HH}} = 8.8$ Hz, $\text{H}^{8\text{a}}$), 1.84 [s, 15H, $\text{C}_5(\text{CH}_3)_5$], 1.89 (s, 3H, CH_3^3), 1.92 (s, 3H, CH_3^2), 1.94 (s, 3H, CH_3^4), 1.96 (m, 1H, $\text{H}^{6\text{a}}$), 2.11 (m, 1H, $\text{H}^{6\text{b}}$), 2.24 (s, 3H, NCH_3), 2.27 (d, 3H, $J_{\text{H-ZrH}} = 1.6$ Hz, CH_3^5), 2.81 (br s, 1H, ZrH), 2.98 (m, 1H, $\text{H}^{7\text{b}}$), 3.54 (m, 1H, $\text{H}^{7\text{a}}$). ^{13}C NMR (25 °C, THF-d_8): $\delta = 10.44$, 11.43, 11.58 (each q, $^1J_{\text{CH}} = 125$ Hz, $\text{CH}_3^{2,4}$), 12.32 [q, $^1J_{\text{CH}} = 125$ Hz, $\text{C}_5(\text{CH}_3)_5$], 15.99 (qd, $^1J_{\text{CH}} = 125$ Hz, $J_{\text{C-ZrH}} = 6.5$ Hz, CH_3^5), 21.68 (t, $^1J_{\text{CH}} = 127$ Hz, CH_2^6), 47.86 (t, $^1J_{\text{CH}} = 140$ Hz, CH_2^8), 52.39 (q, $^1J_{\text{CH}} = 136$ Hz, NCH_3), 68.43 (t, $^1J_{\text{CH}} = 137$ Hz, CH_2^7), 108.03, 109.42, 111.89, 115.66, 119.22 (each s, C^{1-5}), 113.28 [s, $\text{C}_5(\text{CH}_3)_5$]. ^1H NMR (25 °C, C_6D_6): $\delta = 0.21$ (d, 1H, $^2J_{\text{HH}} = 8.8$ Hz, $\text{H}^{8\text{b}}$), 1.36 (d, 1H, $^2J_{\text{HH}} = 8.8$ Hz, $\text{H}^{8\text{a}}$), 1.81, 1.92, 1.98 (each s, 3H, $\text{CH}_3^{2,4}$), 1.91 [s, 15H, $\text{C}_5(\text{CH}_3)_5$], 1.73–1.96

(m, 2H, CH_2^6), 2.18 (s, 3H, NCH_3), 2.41 (d, 3H, $J_{\text{H-ZrH}} = 2.0$ Hz, CH_3^5), 2.75 (m, 1H, $\text{H}^{7\text{b}}$), 3.09 (br s, 1H, ZrH), 3.40 (m, 1H, $\text{H}^{7\text{a}}$). $^{13}\text{C}\{^1\text{H}\}$ NMR (25 °C, C_6D_6): $\delta = 10.32$, 11.36, 11.39 ($\text{CH}_3^{2,4}$), 12.25 [$\text{C}_5(\text{CH}_3)_5$], 16.02 (CH_3^5), 21.24 (CH_2^6), 47.58 (CH_2^8), 51.96 (NCH_3), 67.79 (CH_2^7), 107.63, 109.08, 111.44, 115.26, 118.60 (C^{1-5}), 112.95 [s, $\text{C}_5(\text{CH}_3)_5$]. EI MS (70 eV) m/z (%): 417 (42.0) $[\text{M}]^+$, 401 (40.0) $[\text{M} - \text{CH}_4]^+$, 359 (34.9) $[\text{M} - \text{CH}_2\text{N}(\text{CH}_3)_2]^+$, 147 (3.4) $[\text{C}_7\text{H}_3(\text{CH}_3)_4]^+$, 134 (15.5) $[\text{C}_5(\text{CH}_3)_4=\text{CH}_2]^+$, 133 (16.6) $[\text{C}_7\text{H}_4(\text{CH}_3)_3]^+$, 119 (45.0) $[\text{C}_7\text{H}_5(\text{CH}_3)_2]^+$, 105 (20.2) $[\text{C}_7\text{H}_6(\text{CH}_3)]^+$, 91 (26.2) $[\text{C}_7\text{H}_7]^+$, 59 (6.1) $[\text{N}(\text{CH}_3)_3]^+$, 58 (100) $[\text{CH}_2\text{N}(\text{CH}_3)_2]^+$, 42 (20.4) $[\text{CHNCH}_3]^+$.

3.4. $[\eta^5:\eta^2(C,N)\text{-C}_5(\text{CH}_3)_4\text{CH}_2\text{CH}_2\text{N}(\text{CH}_3)\text{CH}_2\text{-}][\eta^5\text{-C}_5(\text{CH}_3)_5\text{ZrCl}$ (**3**)

To a solution of **2** (77 mg, 0.184 mmol) in THF (2 ml) a 1.5 mol excess of NH_4Cl (15 mg, 0.280 mmol) was added. The reaction mixture was stirred at ambient temperature during 3 h. Gas evolution was observed (appearance of non-condensable components in the reaction vessel). The solution was then separated by decantation, and the residual solid washed three times with THF (2 ml). The combined extracts were concentrated till dryness on the high-vacuum line and the rest recrystallized from ether (2 ml) that gave complex **3** (60 mg, 0.132 mmol, 72%) as colorless crystals. ^1H NMR (25 °C, THF-d_8): $\delta = 0.67$, 1.82 (each d, 1H, $^2J_{\text{HH}} = 9.0$ Hz, CH_2^8), 1.79 [s, 15H, $\text{C}_5(\text{CH}_3)_5$], 1.80, 1.86, 1.98, 2.00 (each s, 3H, $\text{CH}_3^{2,5}$), 2.12 (s, 3H, NCH_3), 2.13, 2.38 (each m, 1H, CH_2^6), 2.95, 3.55 (each m, 1H, CH_2^7). ^{13}C NMR (25 °C, THF-d_8): $\delta = 9.70$, 11.31, 12.32, 14.14 [each q, $^1J_{\text{CH}} = 126$ Hz, $\text{CH}_3^{2,5}$], 12.13 [q, $^1J_{\text{CH}} = 126$ Hz, $\text{C}_5(\text{CH}_3)_5$], 21.59 (t, $^1J_{\text{CH}} = 128$ Hz, CH_2^6), 49.05 (q, $^1J_{\text{CH}} = 136$ Hz, NCH_3), 54.83 (t, $^1J_{\text{CH}} = 143$ Hz, CH_2^8), 67.02 (t, $^1J_{\text{CH}} = 137$ Hz, CH_2^7), 110.19, 113.09, 113.50, 123.04, 123.48 (each s, C^{1-5}), 116.97 [s, $\text{C}_5(\text{CH}_3)_5$]. EI MS (70 eV) m/z (%): 451 (39.9) $[\text{M}]^+$, 436 (62.9) $[\text{M} - \text{CH}_3]^+$, 416 (22.0) $[\text{M} - \text{Cl}]^+$, 400 (92.1) $[\text{M} - \text{Cl} - \text{CH}_4]^+$, 259 (27.6) $[(\text{C}_5(\text{CH}_3)_4\text{CH}_2)\text{ZrCl}]^+$, 147 (3.0) $[\text{C}_7\text{H}_3(\text{CH}_3)_4]^+$, 134 (9.5) $[\text{C}_5(\text{CH}_3)_4=\text{CH}_2]^+$, 133 (12.1) $[\text{C}_7\text{H}_4(\text{CH}_3)_3]^+$, 119 (29.6) $[\text{C}_7\text{H}_5(\text{CH}_3)_2]^+$, 105 (14.4) $[\text{C}_7\text{H}_6(\text{CH}_3)]^+$, 91 (20.6) $[\text{C}_7\text{H}_7]^+$, 59 (5.7) $[\text{N}(\text{CH}_3)_3]^+$, 58 (100) $[\text{CH}_2\text{N}(\text{CH}_3)_2]^+$, 42 (17.1) $[\text{CHNCH}_3]^+$. Found: C, 60.80; H, 7.96; N, 3.15%. Calc. for $\text{C}_{23}\text{H}_{36}\text{ClN}_2\text{Zr}$ (453.21): C, 60.95; H, 8.01; N, 3.09.

¹ Elemental analysis routine failed due to an extreme instability of **2** to air and moisture.

3.5. $[\eta^5:\eta^2(C,N)-C_5(CH_3)_4CH_2CH_2N(CH_3)CH_2-]$
 $[\eta^5-C_5(CH_3)_4CH_2CH_2N(CH_3)_2]ZrH$ (**5**)

To a frozen in liq. N₂ solution of **4** (100 mg, 0.183 mmol) in THF (5 ml), P(CH₃)₃ (350 mg, 4.60 mmol) was condensed on a high-vacuum line and excess of Mg/Hg powder (100 mg, 4.14 mmol) was added. The reaction mixture was thawed and stirred during 5 days (initial dark reddish-brown coloration discharged gradually and the solution became virtually colorless). The unreacted magnesium was filtered off, the volatiles removed on the high-vacuum line and the residue taken with hexane (5 ml). On filtering off the precipitated MgCl₂ and reducing the volume down to ca. 1.5 ml, complex **5** was crystallized as colorless solid (53 mg, 0.111 mmol, 61%). ¹H NMR (25 °C, C₆D₆): δ = 0.24, 1.36 (each d, 1H, ²J_{HH} = 8.8 Hz, CH₂⁸), 1.75–1.94 (m, 2H, CH₂⁶), 1.82, 1.92 (6H), 1.93, 1.96, 1.99, 2.01 (each s, 3H, CH₃^{2-4,2'-5'}), 2.16, 2.17, 2.19 (each s, 3H, NCH₃), 2.20 (m, 2H, CH₂⁷), 2.41 (d, 3H, J_{H-ZrH} = 2.0 Hz, CH₃⁵), 2.54–2.64 (m, 2H, CH₂⁶), 2.74, 3.40 (each m, 1H, CH₂⁷), 3.08 (br s, 1H, ZrH). ¹³C{¹H} NMR (25 °C, C₆D₆): δ = 10.42, 11.39, 11.53, 12.05, 12.18, 12.28, 12.39 (CH₃^{2-4,2'-5'}), 16.02 (CH₃⁵), 21.24 (CH₂⁶), 26.39 (CH₂⁶), 45.69 [N(CH₃)₂], 47.43 (CH₂⁸), 52.01 (NCH₃ in the attached substituent), 60.95 (CH₂⁷), 67.83 (CH₂⁷), 107.70, 109.24, 11.48, 112.13, 112.56, 113.58 (2C), 115.29, 115.48, 118.76 (C^{1-5,1'-5'}). EI MS (70 eV) *m/z* (%): 474 (10.2) [M]⁺, 458 (8.8) [M – CH₄]⁺, 416 (2.1) [M – CH₂N(CH₃)₂]⁺, 147 (2.9) [C₇H₃(CH₃)₄]⁺, 134 (12.1) [C₅(CH₃)₄=CH₂]⁺, 133 (16.6) [C₇H₄(CH₃)₃]⁺, 119 (22.7) [C₇H₅(CH₃)₂]⁺, 105 (6.3) [C₇H₆(CH₃)]⁺, 91 (8.8) [C₇H₇]⁺, 59 (4.5) [N(CH₃)₃]⁺, 58 (100) [CH₂N(CH₃)₂]⁺, 42 (3.3) [CHNCH₃]⁺.²

3.6. NMR-monitored reactions of **2** with CH₃I and P(CH₃)₃

NMR-monitored reactions of **2** with CH₃I and P(CH₃)₃ were performed as described above using in both cases 50 mg of **2** (0.119 mmol) and 45 mg (0.592 mmol) of P(CH₃)₃ and 50 mg (0.352 mmol) of CH₃I in THF-d₈ (0.7 ml in both of cases).

3.7. X-ray crystallographic study

X-ray data for isostructural **3** and co-crystallized **2** and **3** were collected on a Bruker SMART CCD diffractometer (graphite-monochromatized Mo K α radiation, 0.71073 Å) using ω scan mode. Experimental intensities were corrected for Lorentz and polarization effects.

Table 2
Crystal and structure refinement data for **3** and co-crystallized **2** and **3**

	3	Co-crystallized 2 and 3
Empirical formula	C ₂₃ H ₃₆ Cl ₁ N ₁ Zr ₁	C ₂₃ H _{36.75} Cl _{0.25} N ₁ Zr ₁
Formula weight	453.20	427.37
Color, habit	Colorless, block	Colorless, block
Crystal size (mm)	0.2 × 0.1 × 0.1	0.3 × 0.2 × 0.1
Crystal system	Tetragonal	Tetragonal
Space group	<i>P4₂/n</i>	<i>P4₂/n</i>
Cell dimensions		
<i>a</i> (Å)	21.9968(6)	22.0334(14)
<i>c</i> (Å)	8.7610(4)	8.6197(8)
<i>V</i> (Å ³)	4239.1(3)	4184.6(5)
<i>Z</i>	–	8
<i>D</i> _{calc} (g cm ⁻³)	1.420	1.357
<i>μ</i> (mm ⁻¹)	0.652	0.563
<i>F</i> (0 0 0)	1904	1808
Temperature (K)	120(2)	110(2)
<i>θ</i> Range (°)	1.31–27.49	1.31–27.00
Index ranges	–28 ≤ <i>h</i> ≤ 28; –28 ≤ <i>k</i> ≤ 18; –11 ≤ <i>l</i> ≤ 11	–28 ≤ <i>h</i> ≤ 28, –23 ≤ <i>k</i> ≤ 28, –9 ≤ <i>l</i> ≤ 11
Reflections collected	25,444	27,240
Independent reflections (<i>R</i> _{int})	4884 (0.0489)	4567 (0.0670)
Data/restraints/parameters	4884/0/245	4567/0/383
Reflections with <i>I</i> > 2σ(<i>I</i>)	3320	3129
Goodness-of-fit on <i>F</i> ²	1.121	0.941
<i>R</i> indices [<i>I</i> > 2σ(<i>I</i>)]	<i>R</i> ₁ = 0.0442, <i>wR</i> ₂ = 0.1133	<i>R</i> ₁ = 0.0391, <i>wR</i> ₂ = 0.0932
<i>R</i> indices (all data)	<i>R</i> ₁ = 0.0745, <i>wR</i> ₂ = 0.1193	<i>R</i> ₁ = 0.0590, <i>wR</i> ₂ = 0.0992
Largest differential peak/hole (e Å ⁻³)	0.569/–0.597	1.064/–0.422

Semi-empirical absorption corrections based on the measurements of equivalent reflections were applied. The structures were solved by direct methods [24] and refined by full matrix least-squares on *F*² [25]. All non-hydrogen atoms were refined with anisotropic thermal parameters. In the structure of co-crystallized **3** and **2**, abnormally high displacement parameters of chlorine atom clearly indicated its partial occupancy. Refinement of occupation factor led to the value 0.25. All hydrogen atoms in the structure of **3** were placed in calculated positions and refined using a riding model. As for co-crystallized **3** and **2**, all hydrogen atoms (including hydride atom H) were found from difference Fourier synthesis and refined isotropically. Occupancy of hydride atom was assumed to 0.75. In the structure of co-crystallized **3** and **2**, essential residual peaks were not observed in the chlorine/hydride area. Details of X-ray structural investigations are listed in Table 2.

4. Supplementary material

Crystallographic data for the structural analysis has been deposited with the Cambridge Crystallographic

² Elemental analysis routine failed due to an extreme instability of **5** to air and moisture.

Data Centre CCDC Nos. 232614 for compound **3** and 232615 for co-crystallized **3** and **2**. Copies of this information can be obtained free of charge from The Director, CCDC, 12 Union Road, Cambridge, CB2 1EZ, UK, fax: (int code) +44 1223 336 033 or email: deposit@ccdc.cam.ac.uk or <http://www.ccdc.cam.ac.uk>.

Acknowledgments

Authors are thankful to Professor J.A.K. Howard and Professor M.Yu. Antipin for an access to X-ray diffraction facilities. A.V.C. is grateful to the grant of The President of the Russian Federation for young scientists (MK-3697.2004.3) and the Royal Society of Chemistry for the RSC Journal Grants for International Authors.

References

- [1] D.P. Krut'ko, M.V. Borzov, R.S. Kirsanov, M.Y. Antipin, A.V. Churakov, *J. Organomet. Chem.* 689 (2004) 595.
- [2] D.P. Krut'ko, M.V. Borzov, L.G. Kuz'mina, A.V. Churakov, D.A. Lemenovskii, O.A. Reutov, *Inorg. Chim. Acta* 280 (1998) 257–263.
- [3] K.I. Gell, J. Schwartz, *J. Chem. Soc., Chem. Commun.* (1979) 244–246.
- [4] K.I. Gell, J. Schwartz, *J. Am. Chem. Soc.* 103 (1981) 2687–2695.
- [5] R. Bortolin, V. Patel, I. Munday, N.J. Taylor, A.J. Carty, *J. Chem. Soc., Chem. Commun.* (1985) 456.
- [6] D.P. Krut'ko, M.V. Borzov, E.N. Veksler, R.S. Kirsanov, A.V. Churakov, *Eur. J. Inorg. Chem.* (1999) 1973–1979.
- [7] F.H. Allen, *Acta Crystallogr., Sect. B* B58 (2002) 380.
- [8] T.V. Lubben, K. Plössl, J.R. Norton, M.M. Miller, O.P. Anderson, *Organometallics* 11 (1992) 122.
- [9] M. Galachov, P. Gomez-Sal, A. Martín, M. Mena, C. Yelamos, *Eur. J. Inorg. Chem.* (1998) 1319–1325.
- [10] H.H. Karsch, K.-A. Schreiber, M. Reisky, *Organometallics* 17 (1998) 5052–5060.
- [11] J. Pflug, A. Bertuleit, G. Kehr, R. Fröhlich, G. Erker, *Organometallics* 18 (1999) 3818–3826.
- [12] C.J. Harlan, B.M. Bridgewater, T. Hascall, J.R. Norton, *Organometallics* 18 (1999) 3827–3834.
- [13] S.B. Jones, J.L. Petersen, *Inorg. Chem.* 20 (1981) 2889.
- [14] F. Liu, B. Du, J. Liu, E.A. Meyers, S.G. Shore, *Inorg. Chem.* 38 (1999) 3228.
- [15] J.E. Bercaw, *J. Am. Chem. Soc.* 96 (1974) 5087–5095.
- [16] R.D. Sanner, J.M. Manriquez, R.D. Marsh, J.E. Bercaw, *J. Am. Chem. Soc.* 98 (1976) 8351–8357.
- [17] J.M. Manriquez, D.R. McAlister, E. Rozenberg, A.M. Shiller, K.L. Williamson, S.I. Chan, J.E. Bercaw, *J. Am. Chem. Soc.* 100 (1978) 3078–3083.
- [18] J.M. Manriquez, D.R. McAlister, R.D. Sanner, J.E. Bercaw, *J. Am. Chem. Soc.* 100 (1978) 2716–2724.
- [19] S.A. Cohen, P.R. Auburn, J.E. Bercaw, *J. Am. Chem. Soc.* 105 (1983) 1136–1143.
- [20] L.B. Kool, M.D. Rausch, H.G. Alt, M. Herberhold, B. Honold, U. Thewalt, *J. Organomet. Chem.* 320 (1987) 37–45.
- [21] K.I. Gell, J. Schwartz, *J. Am. Chem. Soc.* 100 (1978) 2687–2695.
- [22] F.D. Miller, R.D. Sanner, *Organometallics* 7 (1988) 818–825.
- [23] H. Schmidbaur, J. Adlcofer, K. Schwirten, *Chem. Ber.* 105 (1972) 3382–3388.
- [24] G.M. Sheldrick, *Acta Crystallogr., Sect. A* A46 (1990) 467–473.
- [25] G.M. Sheldrick, SHELXL-97, University of Göttingen, Germany, 1997.